Delft University of Technology

Numerical study of interactive ingress of calcium leaching, chloride transport and multi-ions coupling in concrete

Liu, Qing feng; Shen, Xiao-han ; Šavija, Branko ; Meng, Zhaozheng ; Tsang, Daniel C.W. ; Sepasgozar, Samad ; Schlangen, Erik

Important note
To cite this publication, please use the final published version (if applicable).
Please check the document version above.

Numerical study of interactive ingress of calcium leaching, chloride transport and multi-ions coupling in concrete

Qing-feng Liu [a],[*], Xiao-han Shen [a],[b], Branko Šavija [c], Zhaozheng Meng [a],[c], Daniel C.W. Tsang [d], Samad Sepasgozar [b], Erik Schlangen [c]

[a] *State Key Laboratory of Ocean Engineering, School of Naval Architecture, Ocean & Civil Engineering, Shanghai Jiao Tong University, Shanghai, China*
[b] *Faculty of Built Environment, University of New South Wales, Sydney 2052, Australia*
[c] *Delft University of Technology, Stevinweg 1, 2628 CN Delft, the Netherlands*
[d] *Department of Civil and Environmental Engineering, The Hong Kong Polytechnic University, Hong Kong, China*

A B S T R A C T

In circumstances with wastewater and seawater, the behavior of multi-ions including calcium, chloride and others in concrete attracts attention. The present study investigated the multiple mechanisms that could happen under the special field situation above, including calcium leaching, chloride transport and multi-ion coupling. To realize the interactive ingress of multi ions, the simulation method for the processing of the individual mechanisms and the mutual influences is adopted. The distributions of the diversified ions are analyzed with the influence of the interfacial transition zone. The time-spatial distribution of porosity and its evolution mechanisms are investigated by considering the interaction with calcium ions in both pore solution and solid phase. The results indicate that calcium leaching would dominantly speed up chloride transport due to the coarsened pore structure, while the multi ions electrochemical coupling effect would facilitate calcium leaching in the early stage but subtly delay calcium leaching in the later stage.

1. Introduction

The leaching of calcium in concrete happens especially in industrial and municipal wastewater that is abundant of various ions in the solution [1]. The wastewater influence would be a concern in underground sewage pipes, industrial wastewater dams, and from factory effluent emissions. In this research, special concern is focused on the wastewater infrastructures located by the seaside and other chloride-impacted areas, for example, the industrial wastewater discharged by nuclear plants [2–7]. Nuclear power plants are vitally important structures, in which concrete containers are used to store radioactive wastewater and prevent the waste from contaminating the environment. In essence, leaching is a result of the continuous chemical reaction during the hydration of cement inside the concrete, and is due to the phase transition of calcium between compounds and ions [8]. Calcium is one of the most important constituents in the composite of cement hydration products, present in abundant phases such as calcium hydroxide (CH) and calcium silicate hydrates (C-S-H) [9–11]. Due to the difference in the calcium ion concentration between the concrete and the environment, the calcium

ions leach out of the concrete [12–14]. As a result, the leaching process typically causes a loss of calcium in the concrete, including the dissolution of calcium hydroxide and the decalcification of calcium silicate hydrates [15]. This will result in the degradation of the stiffness and strength of the concrete structure [16,17]. In addition, losing calcium ions also causes a reduction of pH in the concrete. This will also be subject to the deoxidation of the passive film layer of steel and subsequent corrosion of steel reinforcement embedded in concrete, which may further cause the deterioration of the concrete structure [18–20].

In practice, it is very common to build nuclear power plants just by sea for several reasons. In this way, the nuclear station may be located away from densely populated areas. In addition, the seaside economy may benefit from the availability of electrical power. Finally, the emission of cooling wastewater can be handled conveniently in a seaside location. However, abundant chlorides are present in seawater, which may affect the durability of the reinforced concrete structure of a nuclear power plant. Chloride ingress is one of the very typical and most serious durability problems of reinforced concrete structures [21–24]. Due to the higher chloride concentration in the environment, especially the

---

marine environment, the chloride ions will penetrate into the concrete interior [25,26], i.e. in the direction opposite of the leaching process. If a sufficient amount of chloride reaches the level of the steel reinforcement, it will cause steel corrosion and the concrete structure may undergo serious deterioration [27]. In addition, due to leaching the porosity of the concrete will also increase, leading to the faster diffusion of other ionic species including chloride ions through the concrete cover [28–31].

In addition, ionic fluxes might also influence the leaching and chloride ingress process. In the case of coupled calcium leaching and chloride ingress, the pore solution of concrete is filled with different ions including Na^+, OH^-, Ca^{2+}, Cl^-, etc [32–37]. These ions all diffuse and migrate in the pores according to their concentration gradient and electrostatic potential [38,39]. While these effects could all be considered separately, interactive effects also do exist between the ions. In order to involve the coupling effects, both the effects of the external applied electric field and the internal electrostatic potential should be taken into account [40,41]. Because in the natural marine environment external electric field does not exist except when artificially applied, in this study, we will only consider the internal potential. The internal electrostatic potential is produced by the dissimilar diffusivity of these various ionic species and the subsequent charge imbalance in concrete pore solution [42,43]. With regard to the consideration of internal electric potential, the coupling of multi-ionic species would be contemplated in the multi-ion transport process.

Numerous studies have been devoted to understanding the calcium leaching process. Ulm et al. studied the chemo-mechanical behavior of the pores and the solution during calcium leaching, which includes elastic deformation and chemical damage [44]. Carde et al. simulated the strength loss and the porosity increase of cement pastes induced by leaching, and found a good correlation between two established models of stress distribution and porosity [45]. Mainguy et al. developed a model for simulating leaching in pure cement paste and mortar, respectively [46]. Also, Kamali et al. used leaching kinetics to evaluate its influence on materials [47], and based on that, Planel et al. studied the size effect of combined leaching and sulfate ingress in cement paste materials [48]. Larrard et al. presented a simplified model of leaching based on the inverse identification of the tortuosity coefficient, and studied the effect of temperature on leaching [49]. Patel et al. studied the microstructure change of cement paste caused by calcium leaching, based on the reactive transport model, and observed that the leaching rate is proportional to the transport ability of microstructures for the ions [13]. Perko et al. did the modelling on the microstructure effects on calcium leaching, and the results show that despite different physical properties and the presence of microcracks, the leaching kinetics remain the same when the soluble phases are the same [50]. On the other hand, numerous studies have focused on chloride and other ionic transport in concrete. Sergi et al. studied the diffusion of chloride and chloride binding phenomena [51]. Li et al. developed a model of chloride ingress in concrete under a saline environment [52,53]. Geiker et al. summarized and validated the analytical models for the prediction of chloride ingress and binding [54]. Song et al. concluded the influencing factors for chloride transport as concrete mix, curing, exposure condition and others [55]. Gluth et al. reported results of a RILEM TC round robin test about the chloride ingress and carbonation influence of alkali-activated concretes [56]. Decker et al. found and validated a new indicator for the rapid chloride migration test which is not sensitive to sulfide contamination and is applicable for common concrete compositions [57]. The authors of this article established a series of models for multi-component ionic transport, and learned about the distribution profiles of different species [42,58–60].

Based on the individual studies on specific durability problems, understandings of the interaction between leaching and other phenomena, i.e. ionic transport in concrete, have been developed. Micheline et al. studied the combined behavior of leaching and the thermodynamic equilibria of chemical composition under aggressive environments [61].

Roziere et al. studied both the influence of leaching and external sulphate attack on concrete, and found that leaching predominates the reactions, and leached portlandite would encourage the sulphate ingress [62]. Yu et al. also did research about the cement-based material under both leaching and external sulphate attack but in the way of numerical method, and the established model provides good predictions for the experimental results [63]. Tang et al., evaluated the influence of leaching on chloride diffusivity in cement-based materials, and concluded that leaching could increase the chloride diffusion rate, and weaken the chloride binding ability [18,64]. Cherif et al. studied the combined influence of leaching and chloride migration on pore structures of blended cement pastes, and quantified the diffusivity of ions and estimated the kinetics of calcium release [36]. Song et al. Studied the calcium leaching behavior in cement pastes which is in the environment of ammonium chloride aqueous solution, using the EIS approach, and the leaching depths were quantitatively estimated [17]. Hemstad et al. investigated the effect of leaching with HCl on chloride binding, and concluded that leaching and low pH are vital for understanding the peaking behavior of chloride profiles [37]. Most recently, Patel et al. established a pore-scale model for the investigation of leaching and carbonation of cement paste, and revealed that carbon content and pH value significantly influence the precipitated calcite layer [14].

Most of the studies discussed above focus on certain phenomena. Therefore, understanding the mechanisms via modelling while considering multi-ions and the multi-phase nature of concrete may be very insightful. In this article, based on the previous studies about leaching and chloride transport, the focus is on the influence of calcium leaching on chloride transport. In addition, the pore structure evolution caused by leaching is quantified and related to the solid-liquid equilibrium between the compound and free calcium ions. Besides, the influence of the interfacial transition zone (ITZ) between cement paste and coarse aggregates has also been taken into account. Most importantly, the impacts of the multi-ions electrostatic potential on calcium leaching are discussed and analyzed in detail. The time and spatial distribution features of electrostatic potential induced by charge imbalance are also incorporated to better illustrate the impact of the multi-ions coupling effect. This work is implemented in a three-phase model of concrete, which considers the mortar, aggregate and ITZ. In different zones, the transport properties for each species change, the coupling effects also vary, and so do the leaching and the chloride transport process. The results of the present study would be of use for the durability design for the infrastructures in the special engineering environment including wastewater and seawater which contains abundant charged particles like calcium ions and chloride ions.

2. Internal mechanism study

The coupled ingress mechanism of concrete is a complete system. As we are focusing on the combined results of leaching and chloride ingress, together with the multi-ion coupling, we need to deal with each of them, find the key values to relate them, and finally establish a systematic description of the phenomenon.

The mechanisms of the whole process are demonstrated in Fig. 1. The concrete structure exposed to deionized water and contaminated wastewater is facing several corrosion challenges, and these durability problems also influence each other. As shown at the bottom of Fig. 1, the chloride and sodium ions intrude from the concrete surface. In the liquid phase, the intruded chloride ions permeate deeper until reaching the steel reinforcement and initiating corrosion (although some chloride ions will be bound by the solid phase). Besides, electrostatic couplings among multiple ionic species are present. On the other hand, the calcium ions leach out of the concrete due to the low calcium concentration outside, and the equilibrium between the calcium concentration in the liquid phase and the solid phase would lead the solid-phase calcium to dissolve into the pore solution. That would cause the degradation of the concrete, and also widen the transport route for (other) hazardous ions
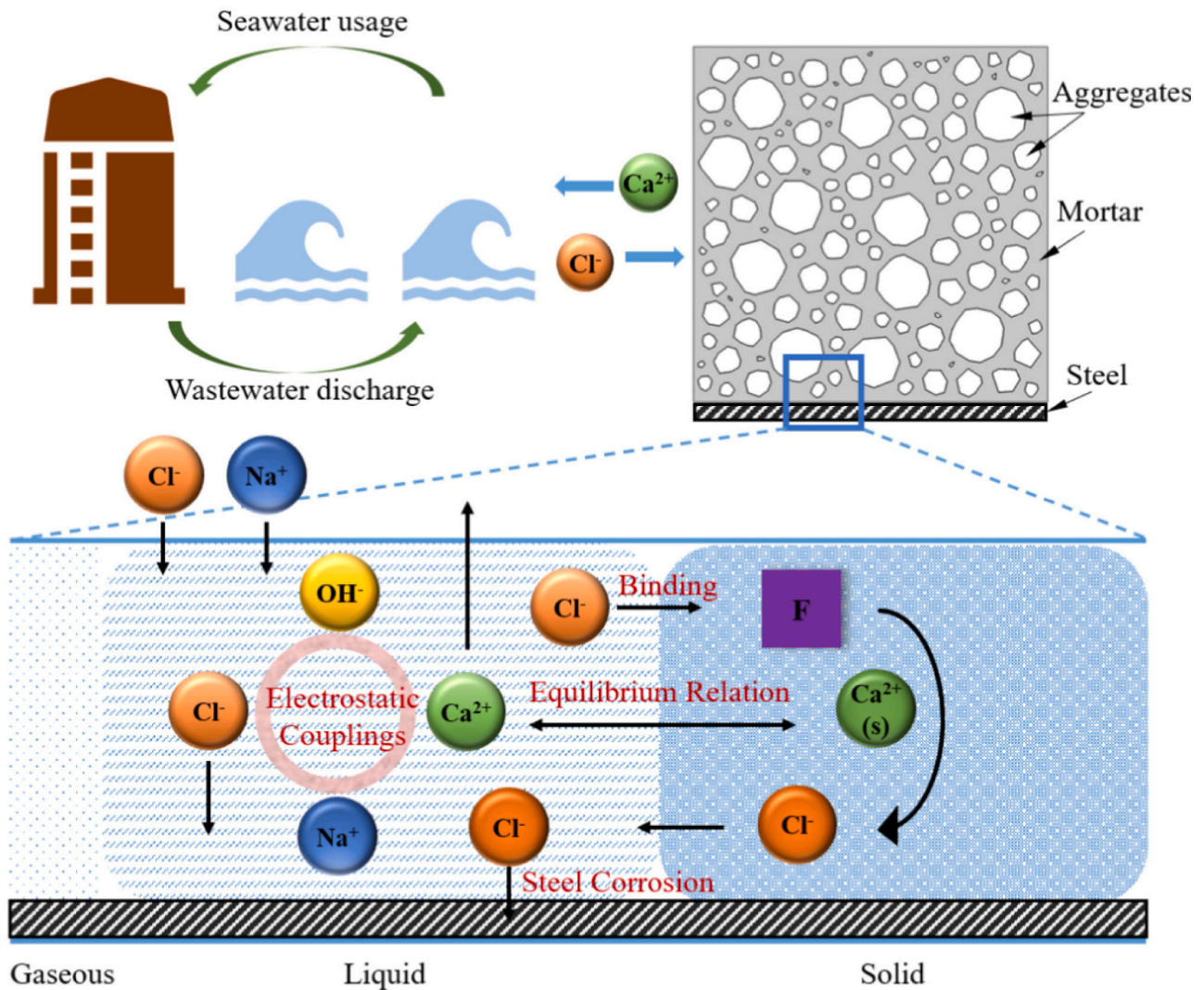
Fig. 1. Mechanisms of combined calcium leaching, chloride transport and multi-ion couplings.

such as chloride to reach the steel reinforcement surface and further aggravate the corrosion. It should be noted that most concrete is in unsaturated condition in practical engineering. However, in terms of calcium leaching which is commonly observed when concrete directly exposed to wastewater, it is the submerged zone that most likely suffers from leaching. Therefore, this study mainly focuses on the saturated condition which is also the condition with the most serious calcium leaching attack.

The whole system mainly utilizes the Nernst-Planck equation to study the transport process of calcium and chloride ions, while separately using the mass balance equation to consider the equilibrium of calcium ions and the chloride binding. In this system, we also evaluated the influence of multi-ion coupling. The conventional Poisson-Boltzmann equation is utilized to consider the interactive electrostatic effects of ionic transport. The calcium leaching process and the chloride binding process are coupled together through the porosity change, so the coupling between these two phenomena is considered through both the porosity and the ionic coupling.

2.1. Calcium leaching and dissolution-precipitation balance

Concrete structures in wastewater face the low-calcium concentration situation, and the concentration gradient leads to the one-dimensional transport of calcium ions from the interior to the exterior,

which is defined as calcium leaching. Besides, the equilibrium between calcium and hydroxide also influences the calcium leaching process, once the concentration of either ion changes, the relationship of them would force the development. The calcium leaching speed could be affected by the temperature, relative humidity, the concentration of calcium ions, pH and etc. In this study, the environmental factors are not the major influencing ingredients here which are not considered in detail. First of all, the calcium leaching process is described with the mass balance equation and Fick's second law is expressed as follows.

$$\frac{\partial C_{f-Ca}}{\partial t} + \frac{\partial C_{s-Ca}}{\partial t} = \varphi \bullet D_{Ca} \frac{\partial^2 C_{f-Ca}}{\partial x^2} \tag{1}$$

where C_{f-Ca} and C_{s-Ca} represent the free and solid calcium concentrations in cement paste respectively. φ describes the porosity of cement paste that influenced by the solid phase of calcium compounds, which is used as $\varphi = 0.589 - 3.3 \times 10^{-5} C_{s-Ca}$ [18]. As can be noticed, the porosity is not set as a constant in the numerical model but a variable which is dependent on the calcium leaching condition. In this way, the influence of porosity variation caused by leaching on the ionic transport behavior can successfully be considered. D_{Ca} represents for the diffusion coefficient of free calcium ions in cement pore solution. The relationship between the solid phase calcium and free-ion calcium concentration under normal temperature and humidity is based on the chemical

reaction transition among different phases of calcium, which could be described as follows,

$$C_{S-Ca} = f(C_{f-Ca}) \tag{2}$$

in detail,

$$f(C_{f-Ca}) = C_{CSH0}\left(\frac{C_{f-Ca}}{C_{st}}\right)^{\frac{1}{3}}(aC_{f-Ca}{}^3 + bC_{f-Ca}{}^2 + c) + d(C_{f-Ca} - q)^3 \tag{3}$$

where,

$$\begin{cases} a = -\dfrac{2}{p^3}, b = \dfrac{3}{q^2}, c = 0, d = 0, & 0 \le C_{f-Ca} < p \\[2mm] a = 0, b = 0, c = 1, d = 0, & p \le C_{f-Ca} < q \\[2mm] a = 0, b = 0, c = 1, d = \dfrac{C_{CH0}}{(C_{st}-q)^3}, & q \le C_{f-Ca} < C_{st} \end{cases} \tag{4}$$

where, C_{CSH0} and C_{CH0} are the initial concentration of C-S-H and calcium hydroxide in cement paste, which has been taken as 7260 mol/m^3 and 3976 mol/m^3; p and q are the boundary concentration of free calcium ions when C-S-H leached completely and C-S-H started leaching after calcium hydroxide dissolved, respectively, and have been set as 2 mol/m^3 and 19.15 mol/m^3 [65]; C_{st} is the initial concentration of free calcium chloride in saturated pore solution of cement paste; The units and values of the above parameters will be described in detail in Table 2.

2.2. Chloride ingress and binding

The chloride ingress and the binding are expressed by the mass balance equation and Fick's second law as follows [66],

$$\frac{\partial C_{f-Cl}}{\partial t} + \frac{\partial C_{s-Cl}}{\partial t} = \varphi \bullet D_{cl}\frac{\partial^2 C_{f-Cl}}{\partial x^2} \tag{5}$$

where C_{f-Cl} is the free chloride concentration in pore solution of cement paste, C_{s-Cl} is the bound chloride concentration in cement paste. D_{cl} represents for the diffusion coefficient of free chloride ions in cement paste. φ was introduced in Section 2.1, which is the porosity of cement paste and evolves according to the calcium equilibrium.

The relationship between the bound chloride and the free chloride is adopted as a binding isotherm in this study as follows,

$$C_{s-cl} = \frac{\beta\alpha C_{f-Cl}}{1 + \alpha C_{f-Cl}} + \gamma C_{f-Cl}^\tau \tag{6}$$

where α, β, γ and τ are empirical constants: α and β are the experimental parameters related to the adsorption at the surface area of free CSH gel, which have been determined as 0.075 and 1.64; γ and τ represent the empirical parameters related to the chemical reactions of the AFm phase, which have been quantified as 0.44 and 0.58 respectively by Carrara et al. [67]. When considering the desorption of previously bound chloride caused by calcium leaching, the binding equation should be revised as

$$C_{s-cl} = \eta_{CSH}\frac{\beta\alpha C_{f-Cl}}{1 + \alpha C_{f-Cl}} + \eta_{CH}\gamma C_{f-Cl}^\tau \tag{7}$$

where η_{CSH} and η_{CH} characterize the remaining amount of CSH and CH respectively, and can be determined as

$$\eta_{CSH} = C_{CSH}/C_{CSH0} \tag{8}$$

$$\eta_{CH} = C_{CH}/C_{CH0} \tag{9}$$

2.3. Multi-ions coupling

It has been acknowledged that in concrete pore solution, other ionic species such as sodium and hydroxyl ions also exist. Because of the charge imbalance induced by different diffusivities and charges of various ionic species, an electrostatic potential would be generated and further impact the ionic transport behavior. As a result, in addition to the diffusion behavior depicted by Fick's second law as shown in Eq. (1) and Eq. (5), the contribution of ionic migration from the multi-ions coupling effect should also be taken into account. In order to consider the multi-component electrolyte inside the pore solution including calcium, sodium, chloride and hydroxyl, the transport of the ions and the electrostatic potential are involved. Based on Fick's second law and the Nernst-Planck equation, the transport of ionic species could be considered as follows

$$\frac{\partial C_{f-i}}{\partial t} + \frac{\partial C_{s-j}}{\partial t} = \varphi \bullet D_i\frac{\partial^2 C_{f-i}}{\partial x^2} + \nabla \bullet D_i z_i C_i\frac{F}{RT}\nabla\varnothing \tag{10}$$

$$i = 1, 2, 3, 4 \ ; j = 1, 2$$

where, i is the i-th ionic species, which respectively represents calcium, sodium, chloride and hydroxyl, while j is the j-th ionic species, in this case representing calcium and chloride in the solid phase; z_i is the charge number for each component; F is the Faraday constant, which is 9.648×10^{-4} C·mol^{-1}; R is the ideal gas constant (8.314 J mol^{-1} K^{-1}); T is the absolute temperature in Kelvin; $\varnothing$ is the electrostatic potential. In order to reflect the internal charge imbalance and the multi-component coupling, the constitutive electro-chemistry law with the form of Poisson's equation is adopted herein to determine the electrostatic potential,

$$\nabla^2\varnothing = -\frac{F}{\varepsilon_0\varepsilon_r}\sum_{i=1}^{N}z_i C_i \tag{11}$$

$$i = 1, 2, 3, 4$$

where ε_0 is the vacuum permittivity, and ε_r is the relative water permittivity under certain temperatures Their values are adapted as 8.854×10^{-12} C·V^{-1} m^{-1} and 78.3, respectively. N is the total number of ions considered.

In addition, the solubility equilibrium between calcium ions and hydroxide ions is also worth attention, the relationship between the concentrations of the ions satisfies:

$$C_{Ca} \bullet C_{OH}^2 = K_s \tag{12}$$

where $K_s = 2 \times 10^{-4}$ mol^3/L^3, which represents the product of solubility between these two ions [68]. This calcium – hydroxide equilibrium implicates the pH reduction caused by leaching, and also contributes to the whole multi-ion coupling system.

3. Modelling and benchmark

The specimen in the present model is in the shape of 0.05 m × 0.05 m square. As shown in Fig. 2 which is the simulated cross-section of a concrete block, the concrete specimen is composed of three phases. The irregular polygon represents the aggregates, and the bulk part is the mortar. In addition, the ITZ layer is elaborated as the geographical shape in the model, which is set as the thickness of 40 μm. It should be noted that ITZ thickness is unevenly distributed in real cases and normally ranges from 20 μm to 80 μm [69]. In the numerical model, the ITZ thickness is averaged as 40 μm to avoid element meshing problems. The ionic diffusion coefficients in ITZ are quantified as 5 times larger than those in cement paste, which is relatively conservative to compensate for enlarged ITZ thickness. Ordinary Portland cement (OPC) is used as the matrix material, and the water-cement ratio is 0.55. Note that our geometrical model could generate different distributions and percentages of aggregate volume. The selected section represents the average 2D shape aggregate volume of the present model, which is 45 % for benchmarking. The model assumes that the contaminated water accesses the concrete from the left side of the specimen. Other sides of the concrete are assumed to be sealed with zero flux boundaries. The initial
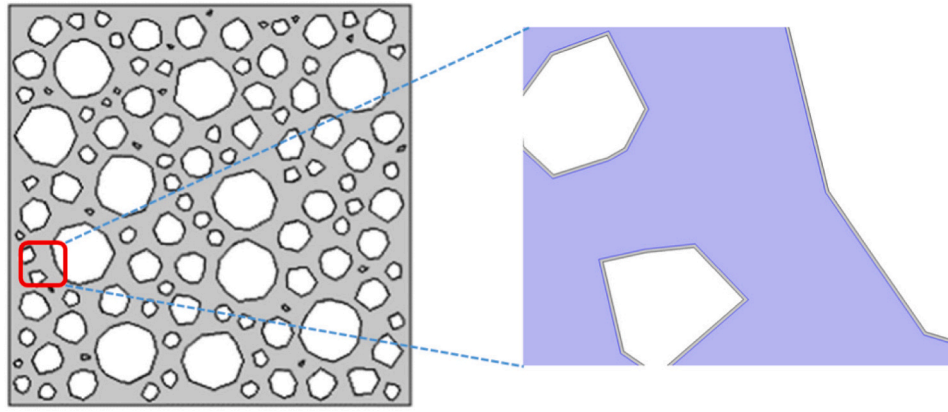
Fig. 2. The cross-section of the specimen used in the model.

concentrations, the boundary concentrations and the initial diffusion coefficients adopted for the benchmark are listed in Table 1. It should be noted that other ions such as sulfate, silicate and potassium also commonly exist in concrete pore solution. However, in order to more explicitly investigate the mutual impact of calcium leaching and chloride ingress, and also considering the relatively lower content of sulfate ions in normal concrete, only chloride, calcium and hydroxyl ions have been included in the presented model. In addition, the governing equations of Eqs. (1), (5) and (10) are solved by the backward difference method and the Newton iteration was adopted to obtain a convergent solution.

The benchmark between the present work and the research of Tang et al. is implemented [18]. It shows the progress of leaching depth with the exposure time changing. In Tang's work, the durability problem of the coupling action of calcium leaching and chloride attack is studied, and it finds that calcium leaching causes higher chloride diffusivity [18]. In this experiment, three kinds of solutions were prepared: 1 mol/L sodium chloride solution, 1 mol/L ammonium chloride solution and the mixed 1 mol/L sodium chloride and 3 mol/L ammonium nitrate solution to compare the leaching behavior. Eighteen specimens were divided into three groups for each solution, cast and cured in the standard order, and then used for the intrusion experiment for the one-dimension diffusion of calcium and chloride ions. After 10, 20, 30, 40, 50 and 60 days of immersion, the specimens were successively taken out for measurement.

In order to compare the leaching depth of Tang's experimental data and the results of our present model, the same corrosion environments are set. The item of 1 mol/L sodium chloride solution is abandoned as it is the control group, and the leaching depth of this situation is not listed by Tang. The acceleration times for 1 mol/L NH$_4$Cl and 1 mol/L NaCl + 3 mol/L NH$_4$Cl are 20 and 40 respectively. The temperature is set as the room temperature of 25 °C. The time steps are set for 10 days, and 60 days in total.

A comparison between the present work and Tang's experiment is presented in Fig. 3, and the leaching depth is determined as the maximum depth where the calcium hydroxide has been completely depleted during the leaching process, which is identical to what has been

mentioned in the experimental study used for benchmarking [18]. The triangle and the circles dots are the experimental results from Tang et al., which show the leaching depth for each time. The dotted lines represent the modelling results of the present research. It is observed that both lines of leaching tendency of mere ammonium chloride solution and mixed solution fundamentally fit the experimental ones. The lines for the present work are smoother than the experiment results. This is as expected since normally experimental data result in small deviations, while models tend to show "smoother" behaviors.

4. Results and discussion

4.1. Overview

The model of the interactive ingress of leaching and chloride has been established. In order to explore the mechanism of the internal coupling effect of calcium leaching and chloride diffusion, together with the interactive effects of multi-ions, several parameters have been studied. This includes different distributions of multi-ions, porosity change and ITZ. Besides, the values adopted in this section for the parameters are listed in Table 2.

According to the established model, several results are observed. First of all, the concentration profiles of various species are shown in Fig. 4. It includes the profiles of calcium, chloride, sodium and hydroxide ions in the liquid phase after 1500 days' intrusion. The 3-D plot clearly shows the distribution of the ions, the x-axis represents the depth to the exposed surface, and the y-axis shows the exposed surface, and the z-axis is the concentration of the ionic species. The specific distribution regularities are illustrated in the following sections. Note that only individual distribution profiles are demonstrated separately in Section 4.1, the coupled influencing results and mechanisms will be further discussed in the following sections.

4.1.1. Calcium leaching

First of all, calcium leaching is the progress of the calcium ions leach from the internal concrete to the external environment. Fig. 5 illustrates the distribution of calcium ions according to the distance of the depth to the exposed concrete surface. The interactive activities inside the concrete are assumed to last for 1500 days, and for every 300 days, the distribution of the calcium ions is plotted. The initial concentration of calcium ions inside the concrete is 20 mol/m³.

The flat surface where the changing of calcium ions begins is the leaching front. As time passes, the calcium ions are leaching out of the concrete, so the leaching front gradually becomes deeper. When leached for 300 days, the leaching front is at the depth of 14.36 mm to the exposed surface, and after 1500 days, the leaching front has reached 25 mm. More specifically, regarding a typical curve of 600 days of leaching, the leaching front is at the depth of 17.01 mm, and the concentration of

Table 1
The charge numbers, initial and boundary concentrations, diffusion coefficients of multi-ions for benchmark [18,70].

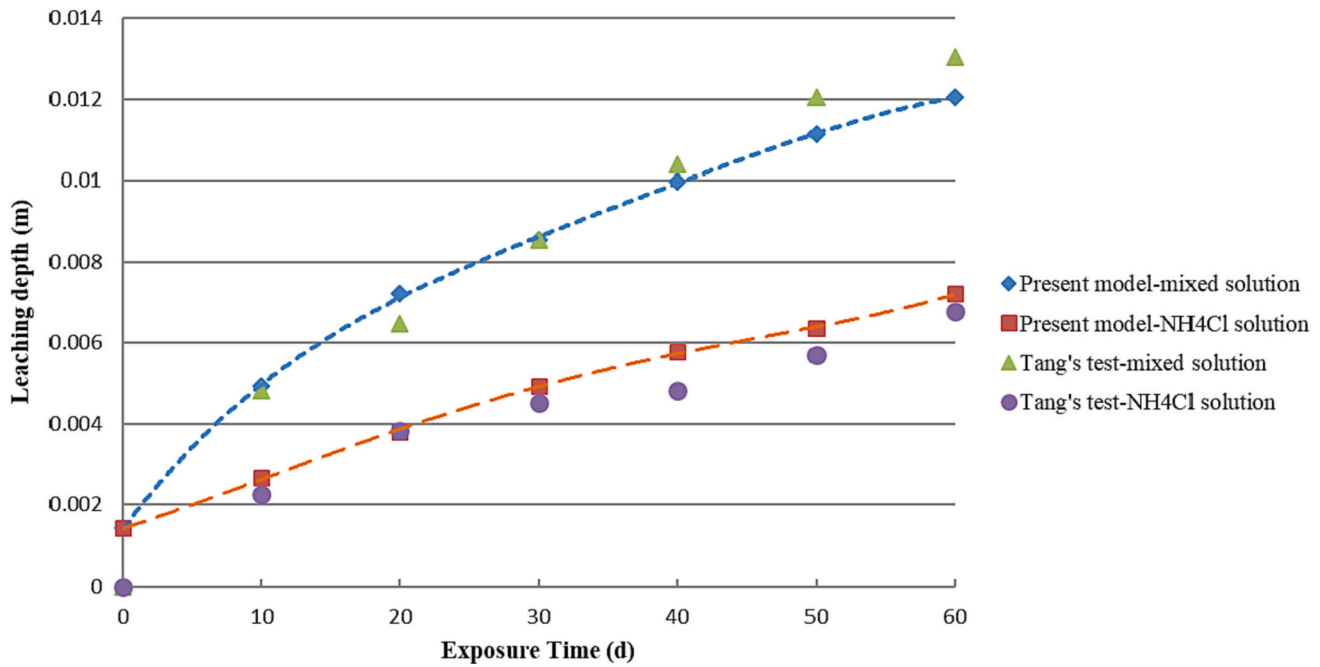| Species	Charge number Z_i	Initial concentration (mol/m³)	Surface concentration (mol/m³)	Diffusion coefficient ($\times 10^{-12}$ m²/s)
Calcium	2	20	0	1.72
Chloride	-1	0	1000	4.41
Sodium	1	40	1000	2.89
Hydroxide	-1	94	0	11.45

Fig. 3. The comparison between the present work and Tang et al.'s experiment.

Table 2
Parameters and values.

Parameters	Abbreviation	Unit	Value
Initial molar volume of CH's calcium ions produced by complete ionization	C_{CH0}	mol/m^3	3976
Initial molar volume of CSH's calcium ions produced by complete ionization	C_{CSH0}	mol/m^3	7260
Initial saturation concentration of calcium ions in the pore solution	C_{st}	mol/m^3	20
The initial concentration of sodium ions in the pore solution	C_{Na0}	mol/m^3	160
The initial concentration of hydroxide ions in the pore solution	C_{OH0}	mol/m^3	200
Boundary concentration of chloride ions	C_{Clb}	mol/m^3	550
Boundary concentration of sodium ions	C_{Nab}	mol/m^3	550
Vacuum permittivity multiplies relative water permittivity	$\varepsilon_0\varepsilon_r$	C·V^{-1} m^{-1}	6.93×10^{-10}
Faraday constant	F	Cmol^{-1}	96,485
Initial porosity	φ_0	–	0.219
Ideal gas constant	R	J mol^{-1} K^{-1}	8.314
Absolute temperature	T	K	298.15
Calcium ion concentration in the pore solution when the CSH gel in the cement-based material is dissolved into silica gel	p	mol/m^3	2
Calcium ion concentration in the pore solution when the CSH gel begins to dissolve after the calcium hydroxide is completely dissolved	q	mol/m^3	19.15
The empirical constant of adsorption isotherm	α	–	0.075
Empirical constant related to dissolution degree of CSH	β	–	1.64
Empirical constant related to the dissolution degree of CH	γ	–	0.44
The empirical constant of chemical binding isotherm	τ	–	0.58

calcium ions falls smoothly from the leaching front to the concrete surface. In the meantime, the distribution of calcium ions becomes more and more gentle. Besides, the leaching speed reduces, as the difference between leaching fronts is decreasing. However, the first 300-day exposure has witnessed the most severe leaching phenomenon, and

the dissolution degree of calcium increases in a milder manner after the first 300 days.

In order to better understand the intrude of the leaching front, Fig. 6 is given. It draws the gradual decrease of the calcium ions in the pore solution from day 0 to day 1500. It shows an obvious leaching-out tendency. Hence, when the leaching front intrudes deeper, the specimen is losing calcium ions, and the total interior amount of calcium ions becomes lower.

4.1.2. Chloride ingress

Fig. 7 shows the distribution of the concentration of chloride ions at different times through the depth of the concrete. The initial concentration inside the concrete is assumed to be 0, and the concentration of chloride ions in the sea water is about 550 mol/m^3. As soon as the chloride ions reach the surface of concrete, the depth is assumed to be chloride contaminated depth. As the exposure time elapses, the chloride intrusion depth moves deeper into the concrete specimen. After 300 days of intrusion, the chloride intrudes to a depth of 15 mm, and after 1500 days of intrusion, the chloride ions reach a depth of more than 25 mm. Speaking of the 600 days intrusion profile, the chloride ions reach the depth of 20 mm, the concentration of chloride ions gradually decreases from the concrete surface to the intrusion front. As time passes, the distribution of chloride ions also becomes gentler. Also, the differences between each intrusion front at different times are decreasing. When the concentration of chloride ions is settled as 200 mol/m^3, the depth differences between 0, 300, 600, 900, 1200 and 1500 days are 7.10, 2.33, 2.09, 0.98, 0.95 mm.

4.1.3. Other ionic species

The distribution of sodium ions according to the time is shown in Fig. 8. The initial sodium concentration in the seawater is 550 mol/m^3, and the initial sodium concentration in concrete is 160 mol/m^3. It is noted that the distribution of sodium ions is coordinated with the chloride ions. After the specimen going through 600 days' intrusion by the simulated seaside, the sodium ions show an almost linear distribution from the highest concentration to the initial interior concrete concentration, from the concrete surface to the depth of 20 mm, while a sudden change appears near the depth that the concentration of sodium ions gradually approach 160 mol/m^3. As the exposure time increases,
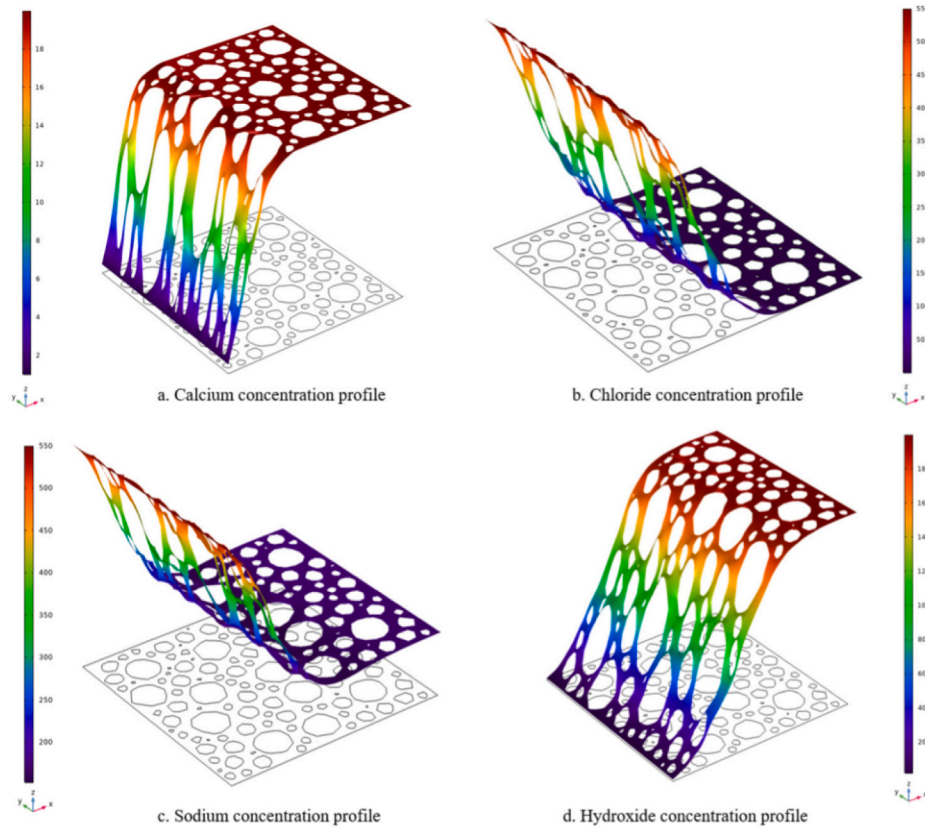
a. Calcium concentration profile

b. Chloride concentration profile

c. Sodium concentration profile

d. Hydroxide concentration profile

Fig. 4. Concentration distribution profiles of multi-species at 1500 days.
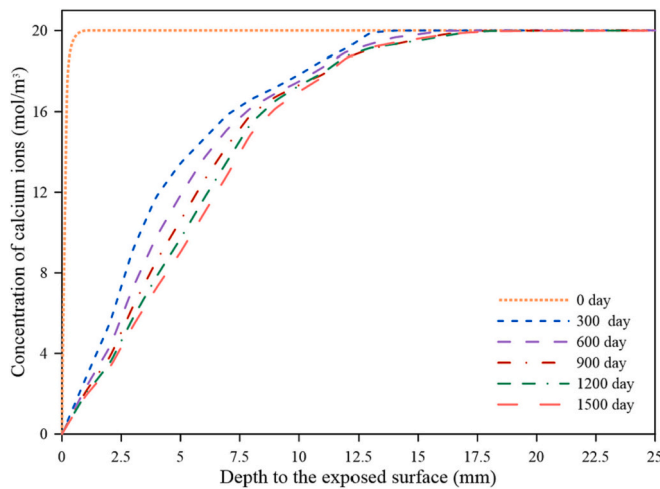

Fig. 5. The distribution of calcium ions concentration with time.

the changing corner of the sodium ion concentration happens later. Furthermore, the differences between the depths are also decreasing.

Fig. 9 shows a distribution of hydroxide ions with time. The initial concentration inside the concrete is assumed to be 200 mol/m³, and the concentration in the environment is assumed to be zero. The distribution of hydroxide ions is a reverse intrusion tendency. It can be seen from Fig. 9 that the hydroxide ions inside the concrete gradually leach out and the pH value decreases accordingly, which has a negative effect on the concrete specimen. Taking the 600 days of exposure as an example, the leaching depth of hydroxide ions has reached 25.94 mm, from the surface to the depth, the distribution of the hydroxide ions concentration shows a gradually increasing trend, and ends up with the sudden change

corner which approaches to 200 mol/m³. After 300 days' intrusion, the hydroxide ions at the depth of 15.83 mm have begun to lose, and after 1500 days' intrusion, the losing depth reaches over 30 mm. Compared to the calcium leaching process, the hydroxide ion leaching speed is faster due to the influence of sodium ions and the coupling effects. Also, as time passes, the differences between the leaching depths are smaller, which means that the leaching speed is decreasing.

4.2. Evolution of pore structures

Because calcium leaching and the resultant porosity variations are coupled, it is necessary to analyze the mechanism of pore structure evolution with the consideration of its interaction with calcium ions. In this section, a general and qualitative description of the time and spatial distribution of concrete porosity will be firstly illustrated based on the proposed numerical model. Then, a quantitative description of porosity profiles will be discussed. Detailed analysis will be carried out considering the interaction with calcium ions dissolution from the solid phase.

4.2.1. Time-spatial distribution of porosity

The pore structure evolution caused by calcium leaching is also studied in the presented modelling work. Fig. 10 illustrates the time-spatial distribution of concrete porosity distributions within a 30 mm concrete cover. It can be seen that due to the dissolution of CH and decalcification of C-S-H gel, the porosity of concrete gradually increases from the inside to the exposed surface, and the maximum porosity at the concrete surface can almost reach 0.6. Besides, it can be observed that the porosity variations caused by leaching are gradually not obvious over time, and the most obvious increase occurs in the first 300 days of exposure, as shown in Fig. 10(b). Nevertheless, by scrutinizing Fig. 10(c) ~(f), it can be seen that although the depth of concrete with porosity ranging from 0.38 to 0.35 barely changes in the remaining exposure duration, the depth of concrete with porosity ranging from 0.35 to 0.22
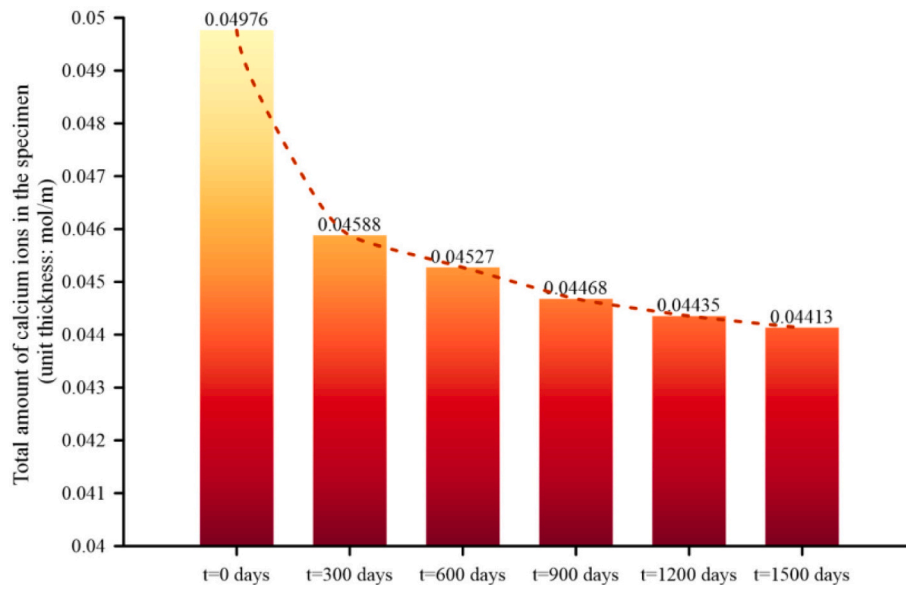
Fig. 6. The changing of the total amount of calcium ions in the specimen (unit thickness).
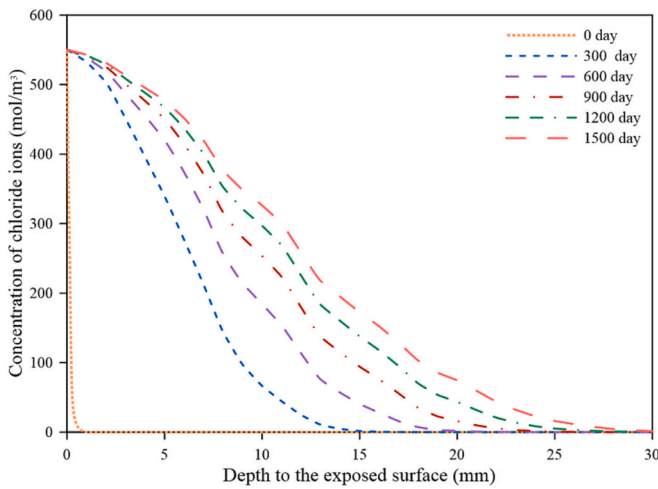

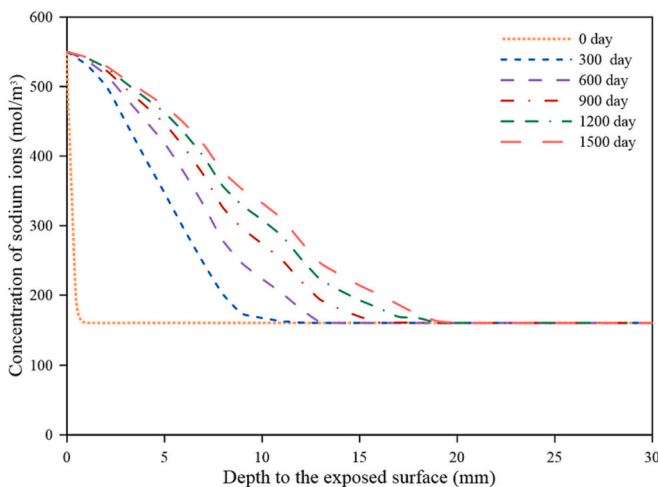**Fig. 7.** The distribution of chloride ions concentration with time.

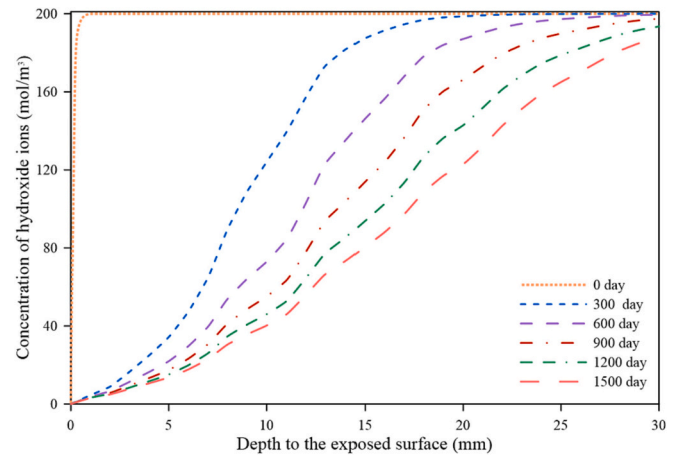**Fig. 8.** The distribution of sodium ions concentration with time.

Fig. 9. The distribution of hydroxide ions concentration with time.

continues to become larger and can almost reach the 30 mm concrete cover after 1500-day exposure, as shown in Fig. 10(f). This indicates that even concrete porosity in the vicinity of steel reinforcement will increase, although slightly, due to the long-term leaching effect, which will fasten the chloride ions penetration to some extent and increase the potential corrosion risk of the embedded reinforcement bar.

4.2.2. Interaction of calcium with pore structures

In order to display the evolution of pore structures from a more quantitative perspective, the porosity variations along concrete cover depth at different exposure times are replotted in Fig. 11. The initial porosity of the concrete specimen is taken as 0.219. The porosity change relates to the change of portlandite, and all ends up the same as 0.591 at the concrete surface. As shown from the curve, after 600 days of exposure, the porosity change reaches the depth of 22.81 mm, the distribution of the porosity change could be generally divided into three parts: in the first part the porosity has a sharp rise from 0.219 to around 0.35, then it turns to grow slowly until around 0.38, after that, it bumps up to 0.591. This is due to the balance between the calcium in the pore solution and in the solid phase, which is illustrated in the following text. After 300 days of chloride ingress and calcium leaching, the porosity change reaches the depth of 16.78 mm, and after 1500 days' intrusion,
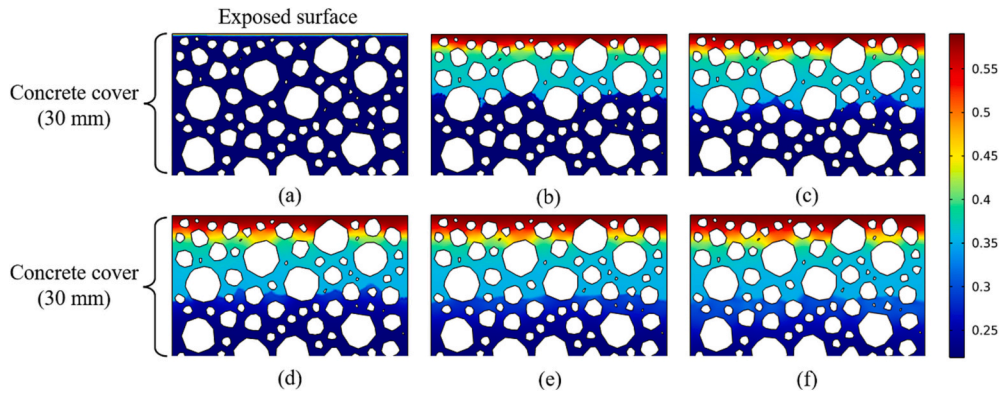
Fig. 10. Time and spatial distribution of concrete porosity under the effect of calcium leaching: (a) 0 day; (b) 300 day; (c) 600 day; (d) 900 day; (e) 1200 day; (f) 1500 day.
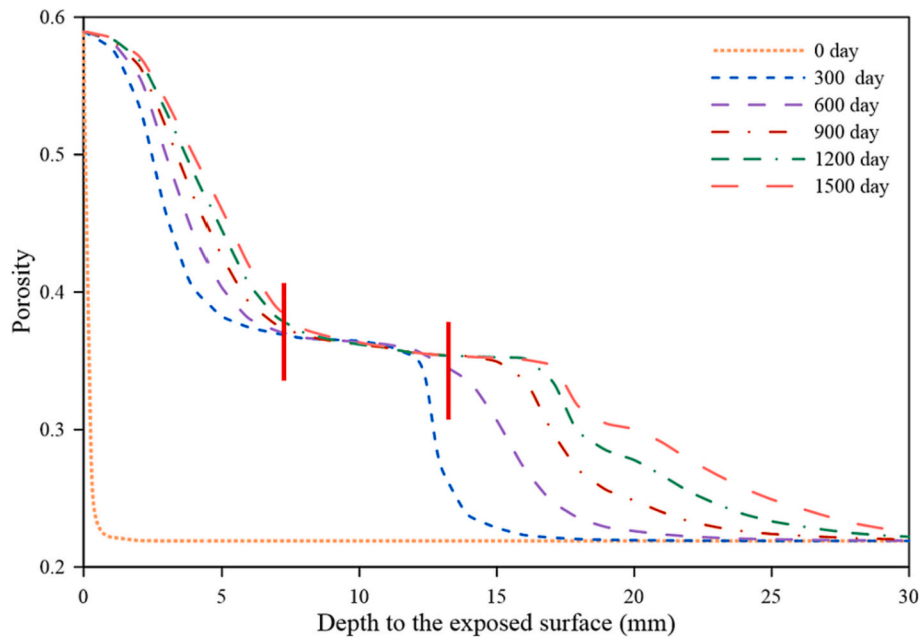

Fig. 11. The pore structure variations along concrete depths at various times.

the porosity change almost reaches the concrete depth of 30 mm.

Furthermore, the concrete pore structures evolution phenomenon can be better understood from its interaction with the calcium ion dissolution from the solid phase. Fig. 12 reveals the relationship between the calcium concentration in the pore solution and the solid phase. For example, when the concentration of calcium ions in the pore solution is 15 mol/m^3, the calcium concentration in the solid phase is around 6600 mol/m^3. The distribution of this equilibrium is also composed of three different parts, that is when the calcium concentration in the liquid is between 0– 2, 2– 19.15 and 19.15– 20. As the porosity changes according to the equilibrium, these three parts of calcium concentration also correlate to the three steps in Fig. 11, for example after 600 days' exposure, the porosity changes between 0.591– 0.38, 0.38– 0.35, 0.35– 0.22. At the changing point of 19.15 mol/m^3 calcium concentration, the calcium hydroxide is completely dissolved and the C-S-H begins to dissolve, in Fig. 11, it is reflected from the exposure depth of 13.5 mm (after 600 days exposure). At the changing point of 2 mol/m^3 calcium concentration, the C-S-H gel in the solid phase is dissolved, which could correlate to the exposure depth of 6.5 mm in Fig. 11 (after 600-day exposure). It shows the changing trends of calcium ions, when the calcium ions leach out of the specimen, the calcium in the solid phase will also reduce to reach the balance. As a

result, the changing tendency of the porosity coordinates with this relationship.

4.3. Influence of ITZ

The interfacial transition zone (ITZ) has different transport properties compared to the diffusivity of the pore solution. Because of the diffusivity differences (see Table 1), the combined intrusion process will also be influenced. Fig. 13 illustrates the contour line of the calcium ions concentration after a 1500-day intrusion, with and without the consideration of ITZ respectively. For example, when the coordinate is selected as (0.004, 0.019) (m), the concentrations for the two situations are on the contour line of 13.5 mol/m^3 and 14.5 mol/m^3, respectively. With the consideration of ITZ, the calcium leaching is faster than when ITZ is not considered. This is because the ITZ part should be treated as a weak layer, where the hazardous ions speed up. As a result, with the consideration of ITZ, the diffusivity of calcium ions also increases, initiating a faster leaching speed.

Fig. 14 illustrates the contour line of the chloride ions concentration after 1500 days of intrusion, with and without the consideration of ITZ respectively. When the coordinate is selected as (0.004, 0.019) (m), the concentrations of the chloride ions are on the contour lines of 178 mol/
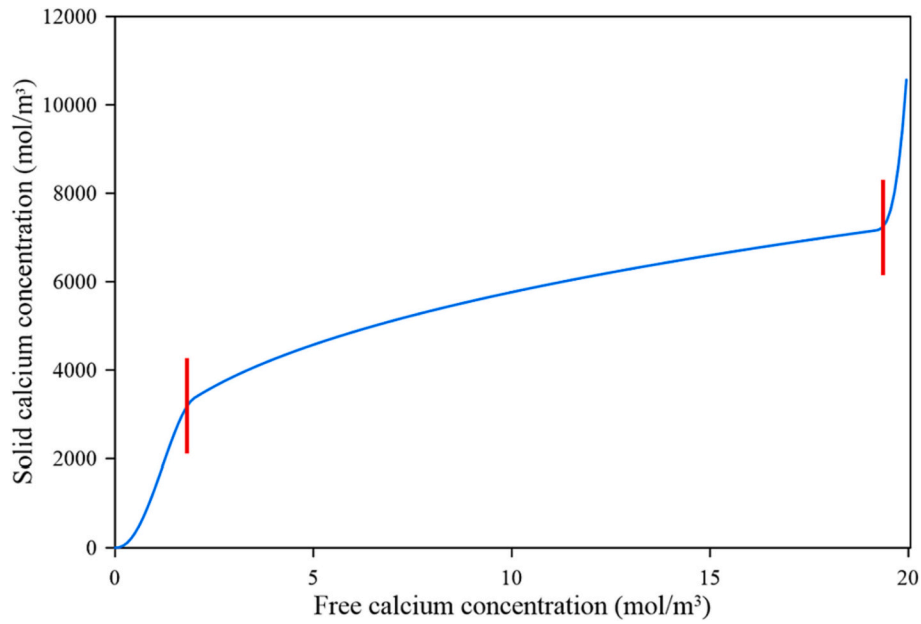
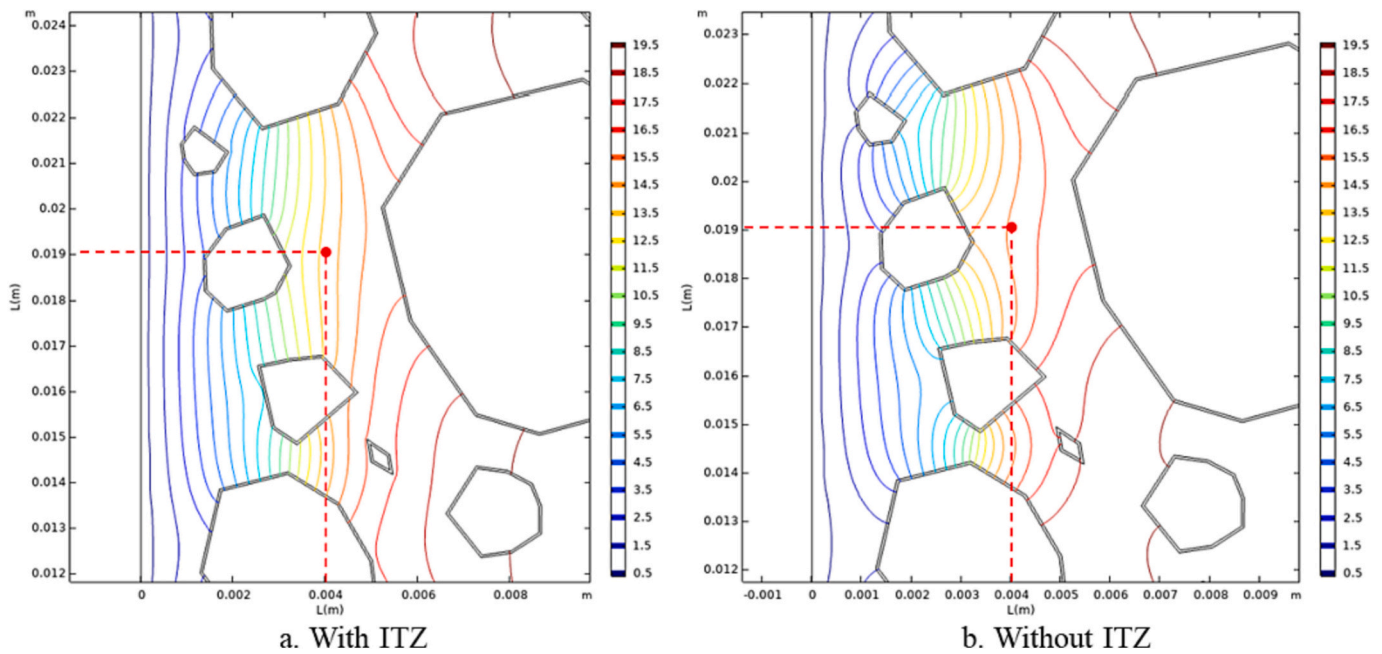**Fig. 12.** The relationship between calcium in pore solution and solid phase.

a. With ITZ

b. Without ITZ

Fig. 13. The contour line of the distribution of calcium ions distribution with and without ITZ.

m^3 and 145 mol/m^3. The selected point belongs to the zone where the chloride ingress has happened but has not been fully chloride-contaminated. As expected, the chloride ingress is also much faster when considering ITZ, which also indicates that with the consideration of ITZ, the corrosion of the rebar is easier to be triggered.

4.4. Influence of calcium leaching on chloride ingress

Fig. 15 shows the chloride distribution in cases when calcium leaching is either considered or not. Different from the dotted lines which show the same distribution as Fig. 7, the solid lines represent the distribution of chloride ions without leaching. It is observed from the graph that the distribution of chloride ions concentration without leaching has the same tendency as those under calcium leaching, while

the transport speed is very different.

It is found from Fig. 15 that the chloride intrusion considering calcium leaching is much faster than that not considering leaching. After 600 days of exposure, the chloride ions without considering leaching reach a depth of 15.62 mm, while the chloride ions with leaching reach a depth of 20.16 mm. After 300, 600, 900, 1200, 1500 days of intrusion, the differences between the reaching depth of chloride ions with and without leaching are 2.42, 4.15, 4.86, 5.57, 6.21 mm, respectively, showing a linearly increasing trend. It is concluded that calcium leaching influence chloride ingress by increasing its' ingress, and this influence becomes greater as time passes, which will accelerate the corrosion process of steel reinforcement. This is attributed to the increased porosity caused by calcium leaching, which can facilitate chloride penetration into concrete cover. This finding typically shows
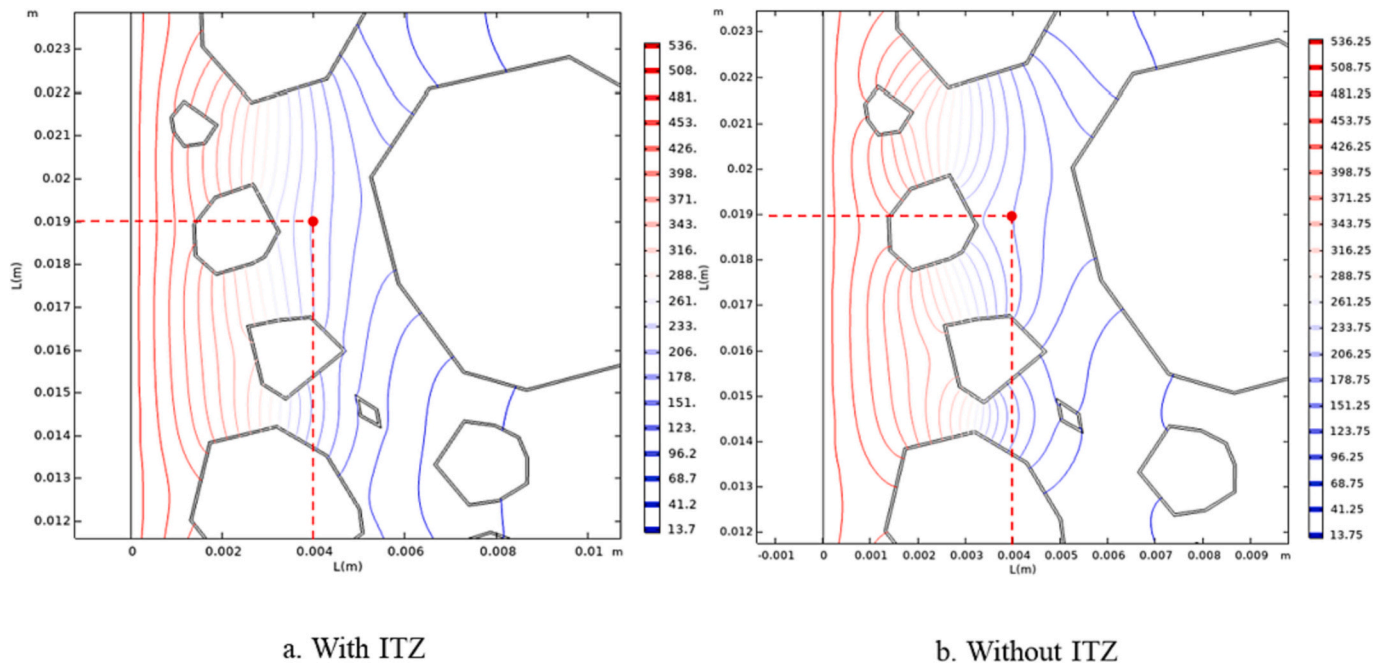
a. With ITZ   b. Without ITZ

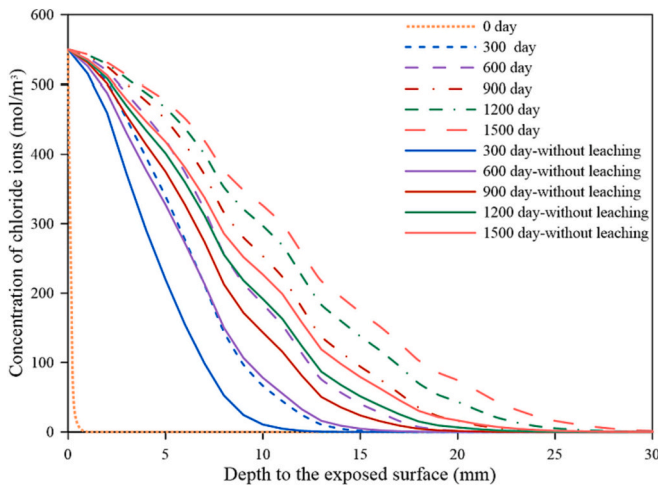**Fig. 14.** The contour line of the distribution of chloride ions distribution with and without ITZ.

Fig. 15. The comparison between the distribution of chloride ions concentration with and without leaching against time.

the importance of the numerical study on the coupling between calcium leaching and chloride ingress.

4.5. Influence of electrostatic potential on calcium leaching

In addition to the influence of calcium leaching on chloride ingress, the penetration of chloride and other ionic species will also impact the calcium leaching process. In detail, with the penetration of chloride from the external environment, a charge imbalance inside concrete pore solution will be generated and cause an electrostatic potential which would influence the ionic transport behavior. Therefore, the transport and concentration distribution of calcium ions will be altered under the impact of the electrostatic potential and the leaching process will also be correspondingly influenced, which also illustrates the importance of considering multi-ion electrochemical coupling effect when modelling calcium leaching. Fig. 16(a)~(e) compares the distribution of calcium ion concentrations with and without the consideration of multi-ions

coupling effect which is associated with the electrostatic potential generated in the transport solution. Fig. 16(f) illustrates the electrostatic potential profiles at the corresponding exposure time in Fig. 16(a)~(e). In terms of time and space, it is shown from the figure that the electrostatic potential caused by charge imbalance gradually decreases over time, and possesses a larger value in the deeper part of the concrete cover.

Before 300 days of calcium leaching, the multi-ionic coupling effect has little influence on the calcium concentration in concrete depths less than 5 mm. This is mainly because the electrostatic potential within the first 5 mm thickness is less than 4 mV, which has little impact on the ionic transport behavior. As for 600- and 900-day exposure, the calcium concentration differences become more obvious from the depth of 7.5 mm. It can also be observed that during the first 600-day exposure, the multi-ions coupling leads to a lower free calcium concentration in deeper depths, which indicates concrete suffers from a more severe leaching phenomenon. This is because the positive electrostatic potential, as shown in Fig. 16(f), will migrate cations including calcium ions away from the inner concrete. Therefore, leached calcium ions in the inner concrete will be partially migrated outward under the action of electrostatic potential, which will enrich the calcium ion in the vicinity of the concrete surface. In this way, the free calcium concentration is lower in deeper concrete depth but conversely higher in the vicinity of concrete cover, as can be observed from Fig. 16(a) to Fig. 16(c). It therefore indicates that models without the consideration of multi-ions coupling will underestimate the leaching degree. However, it can be found that since the 1200-th day, the free calcium ion concentration with the consideration of the multi-ionic coupling effect is generally larger than that without multi-ionic coupling. This can be explained as the leached calcium ions in the inner concrete will be migrated outward under the action of electrostatic potential, which will enrich the free calcium concentration in the outer concrete cover. In addition, it can be seen from the figure that the intersection point between calcium ions concentration with and without multi-ions coupling is gradually shifting towards a deeper depth over time. This phenomenon can be interpreted for the following two reasons: firstly, the smaller electrostatic potential close to the concrete surface leads to a coincidence between cases with and without multi-ionic coupling, and with the increase of electrostatic potential, differences gradually appear to induce different development
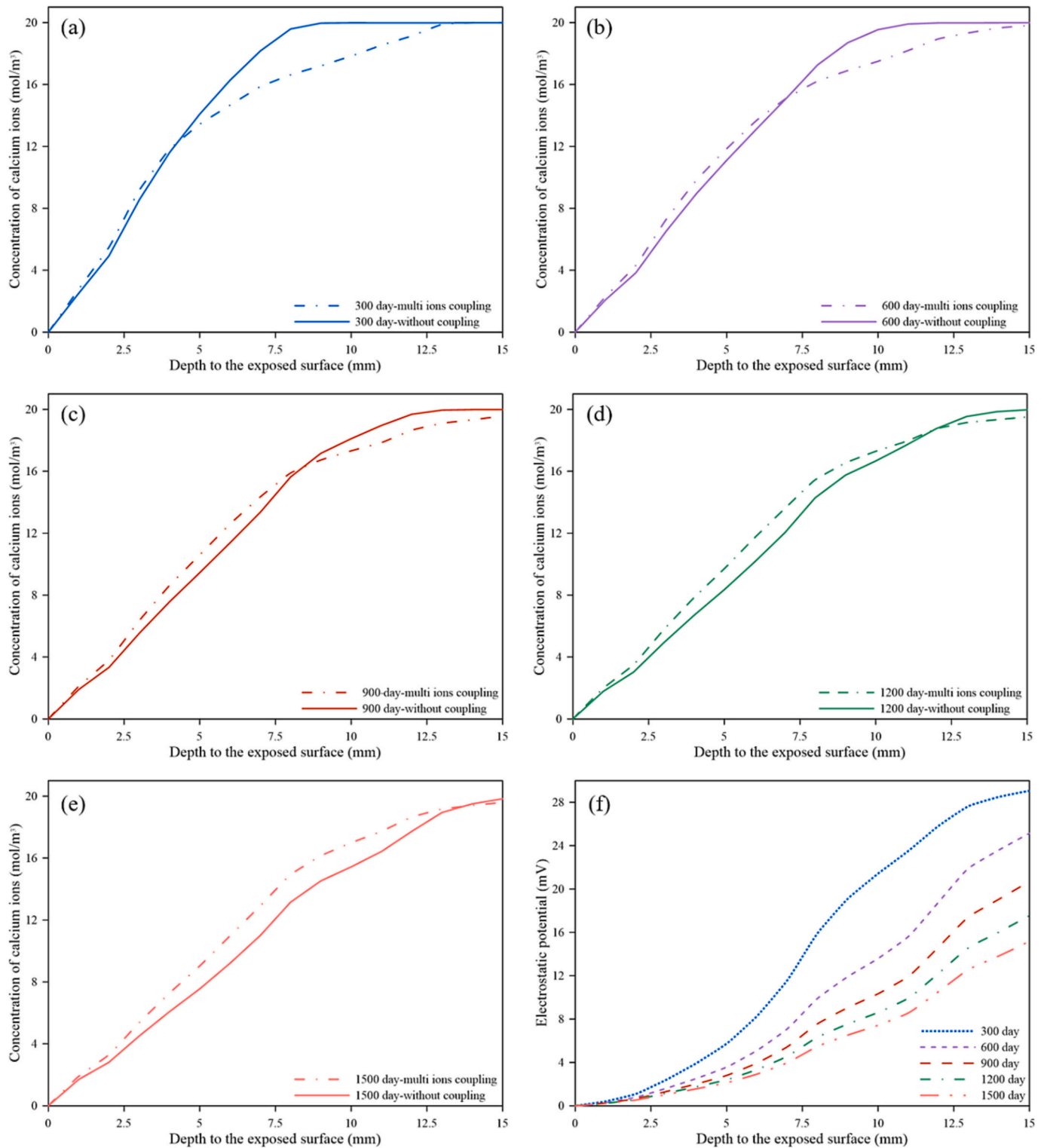
Fig. 16. Calcium ion concentrations with and without multi-ion coupling after (a) 300 days exposure (b) 600 days exposure; (c) 900 days exposure; (d) 1200 days exposure; (e) 1500 days exposure and (f) electrostatic potential profiles at various exposure times.

trends of the two cases. Secondly, the migrated calcium ions lead to the increase of calcium ion concentration at the small depth of concrete, and this results in the moving intersection which moves inward over time.

In order to better illustrate the differences caused by the multi-ions coupling effect, the free calcium ions concentrations in cases with and without the electrochemical coupling effect are compared in Fig. 17(a) and Fig. 17(b) respectively. It can be observed that calcium

concentration profiles without the consideration of the multi-ions effect are almost linear before reaching the leaching front, and remain constant in the deeper concrete depth. On the contrary, calcium concentration distribution under the multi-ions coupling effect is more nonlinear. This can be attributed to the significant influence of electrostatic potential caused by the charge imbalance of various ionic species.
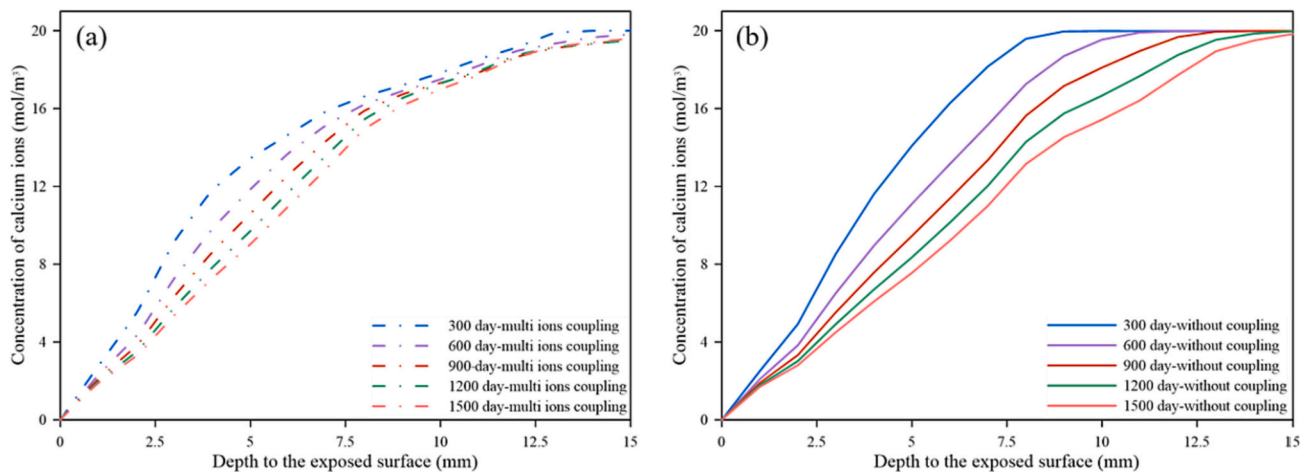
Fig. 17. Comparisons of calcium ion concentrations in cases (a) with multi-ions coupling and (b) without multi-ions coupling effect.

5. Conclusions

With the consideration of the multi-ions electrostatic coupling effect, the research aimed to explore the interactive ingress of calcium leaching and chloride transport. In this process, the concentration distribution of different ions was determined, which is not neglectable. At the same time, the porosity changes of the concrete and the interfacial transition zones influence were analyzed and visualized. In experimental studies, the results show the synergetic influence of all the different individual processes, and the mechanism of each of them is very hard to be measured. While in the present study, the modelling not only learned about the coupling effect, but also included the study of the individual phenomenon. In order to simulate the combined ingress of leaching and chloride, and also the multi-ion coupling, the model including all the mechanisms are built and proves to be reliable. According to the modelling, several conclusion results and contributions are summarized.

1) The performances of various ions under the complex leaching, chloride transport and multi-ion electrochemical coupling situation, corresponding to the normal situation of ions concentration distribution. Calcium ions leach from the concrete to the environment, as time goes by, the leaching front moves deeper, and the leaching speed reduces. Chloride ions intrude into the concrete from the environment, and as time goes by, the intrusion penetrates deeper, and the transport speed reduces. The distribution of other ions coincides with calcium and chloride ions.
2) Due to the dissolution of CH and decalcification of C-S-H gel, calcium leaching leads to an increased concrete porosity. The time-spatial porosity distribution shows that the porosity increases in the direction of calcium leaching, and the porosity near steel concrete surfaces can also get influenced to some extent. When discussing porosity evolution, its interaction with calcium ion concentration cannot be neglected. The change of porosity distribution is related to the equilibrium relationship between calcium ions resolved in pore solution and exists in solid phases. The interfacial transition zone accelerates calcium leaching.
3) The interactive impacts are also studied. It is concluded that calcium leaching accelerates the chloride transport, and this influence becomes more prominent with time. The phenomenon of multi-ion coupling in the process would facilitate calcium leaching in the early stage and subtly slow down calcium leaching in the later stage, and the calcium concentration distribution predicted by considering the electrochemical interactions between multi-species is much more non-linear. These show the significance of modelling work on the coupling among calcium leaching, chloride ingress and electrostatic potential generated by multi-ions.

4) This work considered the special environmental situation while the cement-based material is involved in ions-rich solutions, especially with wastewater and seawater, for example the nuclear plants located by ocean. The findings of this study provide engineering references that can be used as potential solutions for durability problems. In further research, the calcium leaching and chloride transport model with multi-ion coupling are expected to involve more phenomena happen in concrete and cement-based materials, like carbonation and sulfate attack, moisture transport under the unsaturated condition so that the interactive mechanisms and the multi-specie electrochemical effect could be more roundly comprehended.

CRediT authorship contribution statement

Qing-feng Liu: Writing – review & editing, Writing – original draft, Conceptualization, Supervision, Resources, Project administration, Methodology, Funding acquisition. **Xiao-han Shen:** Writing – original draft, Validation, Software, Methodology, Formal analysis, Data curation. **Branko Šavija:** Writing – review & editing, Supervision. **Zhaozheng Meng:** Writing – original draft, Visualization, Investigation. **Daniel C.W. Tsang:** Writing – review & editing, Resources. **Samad Sepasgozar:** Writing – review & editing. **Erik Schlangen:** Writing – review & editing, Resources.

Declaration of competing interest

We declare that we have no financial or personal relationships with other people or organizations that can inappropriately influence our work. There is no professional or other personal interest of any nature or kind in any product, service and/or company that could be construed as influencing the position presented in, or the review of, the manuscript entitled "Numerical study of interactive ingress of calcium leaching, chloride transport and multi-ions coupling in concrete".

Data availability

No data was used for the research described in the article.

Acknowledgments

References

[1] L. Zhang, X. Zuo, Y. Tang, X. Li, Q. Ma, A coupling diffusion model of chloride and calcium ions in hardened cement paste and its numerical simulation, J. Chin. Ceram. Soc. 47 (2) (2019).

[2] B. Gérard, C. Le Bellego, O. Bernard, Simplified modelling of calcium leaching of concrete in various environments, Mater. Struct. 35 (10) (2002) 632–640.

[3] Y.S. Choi, S.Y. Choi, I.S. Kim, E.I. Yang, Experimental study on the structural behaviour of calcium-leaching damaged concrete members, Mag. Concr. Res. 70 (21) (2018) 1102–1117.

[4] Y.-C. Wu, J. Xiao, The effect of microscopic cracks on chloride diffusivity of recycled aggregate concrete, Constr. Build. Mater. 170 (2018) 326–346.

[5] C. Perlot, J. Verdier, M. Carcassès, Influence of Cement Type on Transport Properties and Chemical Degradation: Application to Nuclear Waste Storage, 2005.

[6] Q.T. Phung, N. Maes, S. Seetharam, Pitfalls in the use and interpretation of TGA and MIP techniques for ca-leached cementitious materials, Mater. Des. 182 (2019), 108041.

[7] F. Georget, J.H. Prevost, B. Huet, Reactive transport modelling of cement paste leaching in brines, Cem. Concr. Res. 111 (2018) 183–196.

[8] C. Alonso, M. Castellote, I. Llorente, C. Andrade, Ground water leaching resistance of high and ultra high performance concretes in relation to the testing convection regime, Cem. Concr. Res. 36 (9) (2006) 1583–1594.

[9] L. Liu, X. Wang, J. Zhou, H. Chu, D. Shen, H. Chen, S. Qin, Investigation of pore structure and mechanical property of cement paste subjected to the coupled action of freezing/thawing and calcium leaching, Cem. Concr. Res. 109 (2018) 133–146.

[10] W.-J. Long, T.H. Ye, Y.-C. Gu, H.-D. Li, F. Xing, Inhibited effect of graphene oxide on calcium leaching of cement pastes, Constr. Build. Mater. 202 (2019) 177–188.

[11] W.-J. Long, T.-H. Ye, L.-X. Li, G.-L. Feng, Electrochemical characterization and inhibiting mechanism on calcium leaching of graphene oxide reinforced cement composites, Nanomaterials 9 (2) (2019) 288.

[12] A. Babaahmadi, L. Tang, Z. Abbas, T. Zack, P. Mårtensson, Development of an electro-chemical accelerated ageing method for leaching of calcium from cementitious materials, Mater. Struct. 49 (1–2) (2016) 705–718.

[13] R.A. Patel, J. Perko, D. Jacques, G. De Schutter, G. Ye, K. Van Breugel, A three-dimensional lattice boltzmann method based reactive transport model to simulate changes in cement paste microstructure due to calcium leaching, Constr. Build. Mater. 166 (2018) 158–170.

[14] R.A. Patel, S.V. Churakov, N.I. Prasianakis, A multi-level pore scale reactive transport model for the investigation of combined leaching and carbonation of cement paste, Cem. Concr. Compos. 115 (2020) 103831.

[15] Q.F. Liu, Progress and research challenges in concrete durability: ionic transport, electrochemical rehabilitation and service life prediction, RILEM Tech. Lett. 7 (2022) 98–111.

[16] X. Wang, K. Xu, Y. Li, S. Guo, Dissolution and leaching mechanisms of calcium ions in cement based materials, Constr. Build. Mater. 180 (2018) 103–108.

[17] Z. Song, Y. Liu, L. Jiang, M. Guo, J. Chen, W. Wang, N. Xu, Determination of calcium leaching behavior of cement pastes exposed to ammonium chloride aqueous solution via an electrochemical impedance spectroscopic approach, Constr. Build. Mater. 196 (2019) 267–276.

[18] Y.-J. Tang, X.-B. Zuo, G.-J. Yin, H. Davoudi, X.-N. Li, Influence of calcium leaching on chloride diffusivity in cement-based materials, Constr. Build. Mater. 174 (2018) 310–319.

[19] M. Jebli, F. Jamin, E. Garcia-Diaz, M. El Omari, M.S. El Youssoufi, Influence of leaching on the local mechanical properties of an aggregate-cement paste composite, Cem. Concr. Compos. 73 (2016) 241–250.

[20] C. Zhou, K. Li, X. Pang, Geometry of crack network and its impact on transport properties of concrete, Cem. Concr. Res. 42 (9) (2012) 1261–1272.

[21] Q.-F. Liu, M.F. Iqbal, J. Yang, X.-Y. Lu, P. Zhang, M. Rauf, Prediction of chloride diffusivity in concrete using artificial neural network: modelling and performance evaluation, Constr. Build. Mater. 268 (2021) 121082.

[22] J. Zheng, X. Zhou, Prediction of the chloride diffusion coefficient of concrete, Mater. Struct. 40 (7) (2007) 693–701.

[23] Q.X. Xiong, L.Y. Tong, Z. Zhang, et al., A new analytical method to predict permeability properties of cementitious mortars: the impacts of pore structure evolutions and relative humidity variations, Cem. Concr. Compos. 137 (2023) 104912.

[24] J. Hugenschmidt, R. Loser, Detection of chlorides and moisture in concrete structures with ground penetrating radar, Mater. Struct. 41 (4) (2008) 785–792.

[25] Y. Cai, Q.-F. Liu, Z. Meng, M. Chen, W. Li, B. Šavija, Influence of coarse aggregate settlement induced by vibration on long-term chloride transport in concrete: a numerical study, Mater. Struct. 55 (2022) 235.

[26] Q.F. Liu, Z. Meng, D. Hou, Y. Zhou, Y. Cai, M. Zhang, V.W.Y. Tam, Numerical modelling of electrochemical deposition techniques for healing concrete damaged by alkali silica reaction, Eng. Fract. Mech. 276 (2022) 108765.

[27] Z.Z. Meng, Q.F. Liu, J. Xia, Y.X. Cai, X.J. Zhu, Y. Zhou, L. Pel, Mechanical-transport-chemical modeling of electrochemical repair methods for corrosion-induced cracking in marine concrete, Comput.-Aided Civ. Infrastruct. Eng. 37 (14) (2022) 1854–1874.

[28] L. Cáseres, A. Sagüés, S.C. Kranc, R.E. Weyers, In situ leaching method for determination of chloride in concrete pore water, Cem. Concr. Res. 36 (3) (2006) 492–503.

[29] L.Y. Tong, Q.X. Xiong, M. Zhang, et al., Multi-scale modelling and statistical analysis of heterogeneous characteristics effect on chloride transport properties in concrete, Constr. Build. Mater. 367 (2023) 130096.

[30] W.-Q. Jiang, X.-H. Shen, J. Xia, et al., A numerical study on chloride diffusion in freeze-thaw affected concrete, Constr. Build. Mater. 179 (2018) 553–565.

[31] X.-H. Shen, W.-Q. Jiang, D. Hou, et al., Numerical study of carbonation and its effect on chloride binding in concrete, Cem. Concr. Compos. 104 (2019) 103402.

[32] W.-Q. Jiang, X.-H. Shen, S. Hong, et al., Binding capacity and diffusivity of concrete subjected to freeze-thaw and chloride attack: a numerical study, Ocean Eng. 186 (2019) 106093.

[33] Q.F. Liu, Y. Cai, H. Peng, Z. Meng, S. Mundra, A. Castel, A numerical study on chloride transport in alkali-activated fly ash/slag concretes, Cem. Concr. Res. (2023).

[34] C. Gehlen, S.Von Greve-Dierfeld, K. Osterminsk, Modelling of ageing and corrosion processes in reinforced concrete structures, in: Non-Destructive Evaluation of Reinforced Concrete Structures, Elsevier, 2010, pp. 57–81.

[35] N. Ukrainczyk, E. Koenders, Representative elementary volumes for 3D modeling of mass transport in cementitious materials, Model. Simul. Mater. Sci. Eng. 22 (3) (2014), 035001.

[36] R. Cherif, A.E.A. Hamami, A. Aït-Mokhtar, Effects of leaching and chloride migration on the microstructure and pore solution of blended cement pastes during a migration test, Constr. Build. Mater. 240 (2020), 117934.

[37] P. Hemstad, A. Machner, K. De Weerdt, The effect of artificial leaching with HCl on chloride binding in ordinary Portland cement paste, Cem. Concr. Res. 130 (2020), 105976.

[38] M. Zhang, G. Ye, K. van Breugel, Modeling of ionic diffusivity in non-saturated cement-based materials using lattice boltzmann method, Cem. Concr. Res. 42 (11) (2012) 1524–1533.

[39] L.Y. Tong, Q.X. Xiong, M. Zhang, et al., Modelling the chloride transport in concrete: from microstructure generation to chloride diffusivity prediction, Comput. Struct. (2023).

[40] Z.Z. Meng, Q.F. Liu, W. She, Y.X. Cai, J. Yang, M.F. Iqbal, Electrochemical deposition method for load-induced crack repair of reinforced concrete structures: a numerical study, Eng. Struct. 246 (2021) 112903.

[41] L.-X. Mao, Z. Hu, J. Xia, et al., Multi-phase modelling of electrochemical rehabilitation for ASR and chloride affected concrete composites, Compos. Struct. 207 (2019) 176–189.

[42] Q.-F. Liu, G.-L. Feng, J. Xia, J. Yang, L.-Y. Li, Ionic transport features in concrete composites containing various shaped aggregates: a numerical study, Compos. Struct. 183 (2018) 371–380.

[43] W. Chen, Q. Liu, Moisture and multi-ions transport in concrete under drying-wetting cycles: a numerical study, J. Hydraul. Eng. 52 (5) (2021) 622–632.

[44] F.-J. Ulm, J.-M. Torrenti, F. Adenot, Chemoporoplasticity of calcium leaching in concrete, J. Eng. Mech. 125 (10) (1999) 1200–1211.

[45] C. Carde, R. Francois, Modelling the loss of strength and porosity increase due to the leaching of cement pastes, Cem. Concr. Compos. 21 (3) (1999) 181–188.

[46] M. Mainguy, C. Tognazzi, J.-M. Torrenti, F. Adenot, Modelling of leaching in pure cement paste and mortar, Cem. Concr. Res. 30 (1) (2000) 83–90.

[47] S. Kamali, B. Gérard, M. Moranville, Modelling the leaching kinetics of cement-based materials—influence of materials and environment, Cem. Concr. Compos. 25 (4–5) (2003) 451–458.

[48] D. Planel, J. Sercombe, P. Le Bescop, F. Adenot, J.-M. Torrenti, Long-term performance of cement paste during combined calcium leaching–sulfate attack: kinetics and size effect, Cem. Concr. Res. 36 (1) (2006) 137–143.

[49] T. de Larrard, F. Benboudjema, J.-B. Colliat, J.-M. Torrenti, F. Deleruyelle, Concrete calcium leaching at variable temperature: experimental data and numerical model inverse identification, Comput. Mater. Sci. 49 (1) (2010) 35–45.

[50] J. Perko, N. Ukrainczyk, B. Šavija, Q.T. Phung, E.A. Koenders, Influence of micro-pore connectivity and micro-fractures on calcium leaching of cement pastes—a coupled simulation approach, Materials 13 (12) (2020) 2697.

[51] G. Sergi, S. Yu, C. Page, Diffusion of chloride and hydroxyl ions in cementitious materials exposed to a saline environment, Mag. Concr. Res. 44 (158) (1992) 63–69.

[52] Y. Wang, L.-Y. Li, C. Page, Modelling of chloride ingress into concrete from a saline environment, Build. Environ. 40 (12) (2005) 1573–1582.

[53] L.-Y. Li, D. Easterbrook, J. Xia, W.-L. Jin, Numerical simulation of chloride penetration in concrete in rapid chloride migration tests, Cem. Concr. Compos. 63 (2015) 113–121.

[54] M. Geiker, E.P. Nielsen, D. Herfort, Prediction of chloride ingress and binding in cement paste, Mater. Struct. 40 (4) (2007) 405.

[55] H.-W. Song, C.-H. Lee, K.Y. Ann, Factors influencing chloride transport in concrete structures exposed to marine environments, Cem. Concr. Compos. 30 (2) (2008) 113–121.

[56] G.J. Gluth, K. Arbi, S.A. Bernal, D. Bondar, A. Castel, S. Chithiraputhiran, A. Dehghan, K. Dombrowski-Daube, A. Dubey, V. Ducman, RILEM TC 247-DTA round robin test: carbonation and chloride penetration testing of alkali-activated concretes, Mater. Struct. 53 (1) (2020) 1–17.

[57] M. Decker, R. Grosch, S. Keßler, H. Hilbig, Chloride migration measurement for chloride and sulfide contaminated concrete, Mater. Struct. 53 (4) (2020) 1–11.

[58] Q.-F. Liu, D. Easterbrook, J. Yang, L.-Y. Li, A three-phase, multi-component ionic transport model for simulation of chloride penetration in concrete, Eng. Struct. 86 (2015) 122–133.

[59] Q. Liu, Multi-phase modelling of concrete at meso-micro scale based on multi-species transport, J. Chin. Ceram. Soc. 46 (8) (2018) 1074–1080.

[60] Q.F. Liu, Z. Hu, X.E. Wang, H. Zhao, K. Qian, L.J. Li, Z. Meng, Numerical study on cracking and its effect on chloride transport in concrete subjected to external load, Constr. Build. Mater. 325 (2022) 126797.

[61] M. Moranville, S. Kamali, E. Guillon, Physicochemical equilibria of cement-based materials in aggressive environments—experiment and modeling, Cem. Concr. Res. 34 (9) (2004) 1569–1578.

[62] E. Rozière, A. Loukili, R. El Hachem, F. Grondin, Durability of concrete exposed to leaching and external sulphate attacks, Cem. Concr. Res. 39 (12) (2009) 1188–1198.

[63] Y. Yu, Y. Zhang, A. Khennane, Numerical modelling of degradation of cement-based materials under leaching and external sulfate attack, Comput. Struct. 158 (2015) 1–14.

[64] C. Perlot, M. Carcassès, J. Verdier, Diffusivity evolution under decalcification: influence of aggregate natures and cement type, Mater. Struct. 46 (5) (2013) 787–801.

[65] Q. Ma, X. Zuo, Y. Tang, Numerical simulation of calcium leaching process of hardened cement paste under action of environmental water, Hydro-Sci. Eng. 3 (2017) 107–115.

[66] C.L. Zhang, W.K. Chen, S. Mu, et al., Numerical investigation of external sulfate attack and its effect on chloride binding and diffusion in concrete, Constr. Build. Mater. 285 (2021) 122806.

[67] P. Carrara, L. De Lorenzis, D.P. Bentz, Chloride diffusivity in hardened cement paste from microscale analyses and accounting for binding effects, Model. Simul. Mater. Sci. Eng. 24 (6) (2016), 065009.

[68] L. Li, C. Page, Finite element modelling of chloride removal from concrete by an electrochemical method, Corros. Sci. 42 (12) (2000) 2145–2165.

[69] Z. Hu, L.X. Mao, J. Xia, et al., Five-phase modelling for effective diffusion coefficient of chlorides in recycled concrete, Mag. Concr. Res. 70 (11) (2018) 583–594.

[70] Y.G. Yu, W. Gao, Y. Feng, A. Castel, X.J. Chen, A.R. Liu, On the competitive antagonism effect in combined chloride-sulfate attack: a numerical exploration, Cem. Concr. Res. 144 (2021) 106406.